International Journal of Applied Science; Vol. 8, No. 4; 2025
ISSN 2576-7240 E-ISSN 2576-7259
https://doi.org/10.30560/ijas.v8n4p91

A Comparative Study on the Axial Compression Stability Performance of CFST Columns with Different Cross-Sections: A Meta-Analysis Based on a Unified Benchmark

Shan Shuo[1]

[1] School of Civil Engineering, Chongqing University, China

Correspondence: Shan Shuo, School of Civil Engineering, Chongqing University, Chongqing 400045, China.

Received: November 21, 2025; Accepted: December 4, 2025; Published: December 5, 2025

Abstract

CFST columns are widely used in building structures, and their axial compression stability is a key factor in design. The cross-sectional shape may significantly affect the mechanical properties of the column, but existing studies mostly focus on specific shapes and lack systematic comparisons. Through a meta-analysis, systematically evaluate the axial compression stability performance of CFST columns with different cross-sectional shapes (rectangular, elliptical, circular ring-shaped, and circular) under a unified benchmark, and assess the reliability of the existing prediction models. Through a meta-analysis approach, sample data from numerous experimental and numerical studies were integrated. The core method is to uniformly adjust the "measured bearing capacity/predicted limit" (N_{ue}/N) effect size of all samples to the normalized slenderness ratio λ=0.657 by using the specific slope coefficients of each section. Based on this, descriptive statistical analysis was conducted, and by performing linear fitting on the scatter data, the theoretical stability coefficients of each cross-section at the normalized slenderness ratio λ=1 were extrapolated, and heterogeneity(I^2 statistic) was evaluated. A total of 8 studies were included (providing 142 samples). The mean corrected effect size showed that the prediction models of the circular ring-shaped cross-section (1.078) and the circular cross-section (1.031) had higher reliability, while the prediction values of the rectangular cross-section (0.844) were systematically higher than the measured values. The linear fitting analysis further revealed that when reaching the theoretical buckling critical point (λ=1), the stability coefficients of each cross-section, from highest to lowest, were: circular ring-shaped (0.876), circular (0.848), elliptical (0.779), and rectangular (0.693). The heterogeneity among the studies was relatively high (I^2 > 50%). The cross-sectional shape has a significant impact on the axial compression stability performance of the CFST columns and the accuracy of the prediction model. Under the same condition of normalized slenderness ratio, the circular ring-shaped cross-section exhibits the best stability performance, while the stability performance and model reliability of the rectangular cross-section are the lowest. When conducting structural design, the influence of the cross-sectional shape of the components should be taken into account, and the prediction model should be further verified.

Keywords: CFST column, Axial compression stability, Cross-section, Meta-analysis, Stability coefficient

1. Introduction

Concrete-filled steel tubular columns (CFST columns) combine the advantages of steel and concrete, featuring high strength, good ductility and excellent seismic performance. They are widely used in modern civil engineering projects such as high-rise buildings and bridges[1]. Axial compression stability is the core issue in the design of CFST columns, involving local buckling, overall stability, and material interaction. Different cross-sectional shapes (such as circular, rectangular, circular ring-shaped, elliptical, etc.) result in significant performance differences of CFST columns by altering the concrete confinement effect, stress distribution, and buckling mode[2].

Although a large number of studies have been conducted on CFST columns of specific cross-sectional shapes, due to the different ranges of normalized slenderness ratio of the test specimens used in each study, it is difficult to directly compare and draw conclusions about the performance differences solely caused by the cross-sectional shapes[3]. Meta-analysis, as a statistical method, can integrate the results of multiple independent studies, providing more reliable integrated evidence[4-5]. Therefore, this study employed a meta-analysis. To eliminate the interference of the normalized slenderness ratio, all data were adjusted to a unified reference point. This approach allowed for a clear comparison of the axial compression stability of rectangular, elliptical, circular ring-shaped,

and circular cross-sections. It also evaluated the applicability of existing bearing capacity prediction models for different cross-sections to guide engineering design and further research.

2. Materials and Methods

2.1 Search Strategy for Literature

In databases such as Web of Science, CNKI, Wanfang Data, Engineering Village and Google Scholar, research published up to August 2025 was retrieved using keywords such as "concrete-filled steel tubular columns", "CFST", "axial compression", "cross-section", "rectangular", "elliptical", and "circular".

2.2 Inclusion and Exclusion Criteria

2.2.1 Inclusion Criteria

(1) Experimental or numerical studies; (2) The dimensional parameters of the CFST columns under axial pressure and the measured bearing capacity (N_{ue}); (3) The cross-sectional shapes are rectangular, elliptical, circular, or circular ring-shaped; (4) Provide sufficient data for calculating and predicting the bearing capacity.

2.2.2 Exclusion Criteria

(1) Not axial compression; (2) Seismic resistance, fire resistance, bolts; (3) Repeated publication; (4) Incomplete data or data unable to be extracted.

2.3 Data Extraction and Quality Assessment

Two researchers independently extracted the data, including the paper title, cross-sectional shape, pressure location, measured bearing capacity, predicted limit, normalized slenderness ratio, etc. The quality of the observational study was evaluated using the Newcastle-Ottawa Scale, and any disagreements were resolved through negotiation[6-7].

2.4 Statistic Analysis

Every predicted limit is calculated according to the following formula[8]:

$$N = f_c \times A_c + f_y \times A_s$$

The effect size is the ratio of the measured bearing capacity to the predicted limit (N_{ue}/N). For each cross-sectional shape, the weighted average effect size is calculated using a random effects model to account for the heterogeneity among studies. Heterogeneity was evaluated using the I^2 statistic. $I^2 > 50\%$ indicated significant heterogeneity. All analyses were conducted using Stata software. The confidence interval (CI) was set at 95%.

To conduct a fair comparison, the following two key steps were implemented in this study:

Stability coefficient calculation: Based on the scatter plot formed by the sample data, perform linear regression on each section data to obtain the linear relationship between N_{ue}/N and normalized slenderness ratio λ. By substituting $\lambda = 1$ into the fitting formula, the stability coefficient at the theoretical buckling critical point of each cross-section can be calculated. The scatter plots and linear relationships of different cross-sections are shown in Figure 2.

Effect size correction: For each data point, the N_{ue}/N value is corrected to a uniform normalized slenderness ratio $\lambda_0 = 0.657$ (the average of the normalized slenderness ratios) using the slope coefficients k of the linear regression line of its corresponding cross-sectional scatter plot. The correction formula is:

$$N_{ue} / N_{corrected} = N_{ue} / N_{original} - k \cdot (\lambda - \lambda_0)$$

Among them, the values for the rectangular cross-section are k = -0.44012, for the elliptical cross-section are k = -0.40179, for the circular ring-shaped cross-section are k = -0.46954, and for the circular cross-section are k = -0.42672.

Descriptive statistics (mean, standard deviation, median, etc.) were conducted for the corrected effect size, and the stability coefficient obtained through linear fitting was used as the final key indicator for evaluating the stability performance of each cross-section.

3. Results

3.1 Literature Search Results

The detailed flowchart of the literature screening process is shown in Figure 1. After searching the databases of Web of Science, CNKI, Wanfang Data, Engineering Village and Google Scholar according to the inclusion and

exclusion criteria, 1578 published studies were identified (including 1208 from CNKI, 30 from Wanfang Data, 264 from Google Scholar, 61 from Engineering Village and 15 from Web of Science). After removing duplicate references, 1395 remained. After screening by title/abstract, 1348 studies were excluded.

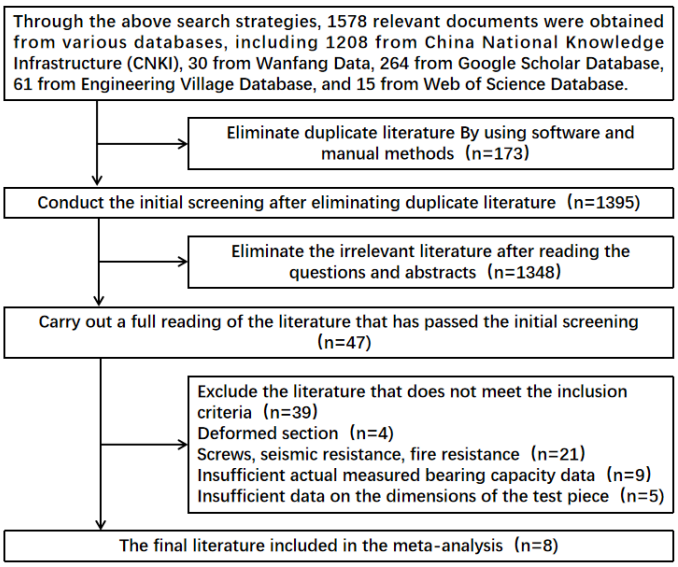

Figure 1. Inclusion flowchart of the literature

Subsequently, a full-text evaluation was conducted on the remaining 47 articles, and 39 of them were excluded as they did not meet the inclusion criteria (4 were of an irregular cross-section; 21 were related to bolts, seismic resistance, and fire resistance; 9 had insufficient measured bearing capacity calculation data; and 5 had insufficient specimen size data). Therefore, a total of 8 articles were included in the final meta-analysis.

3.2 Basic Information of the Research Literature

Based on the inclusion and exclusion criteria set by the research, a total of 8 articles were included in this study. All the included studies were axial compression tests, published between 2001 and 2025. The total sample size of the tests was 142, and the test components included four types of steel tube columns with rectangular, elliptical, circular, and annular cross-sections.

3.3 Article Quality Assessment

A total of 8 articles were included in this study and their quality was evaluated. The heterogeneity test indicated that there was a high degree of heterogeneity among the studies ($I^2 = 93.3\%$, $P < 0.01$) (Figure 2[9-16]). The funnel plot was basically symmetrical (Figure 3), and the overall risk of bias was low (Figure 4). Therefore, the 8 studies included in this article have high quality and the credibility of the article is high.

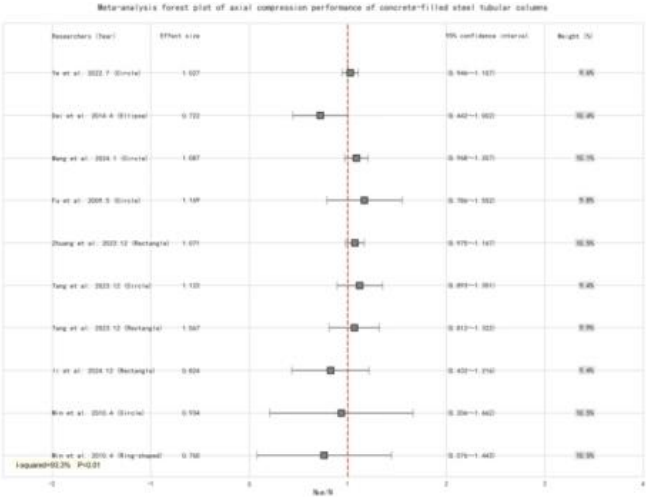

Figure 2. Meta-analysis forest plot of the influence of cross-sectional shape on N_{ue}/N

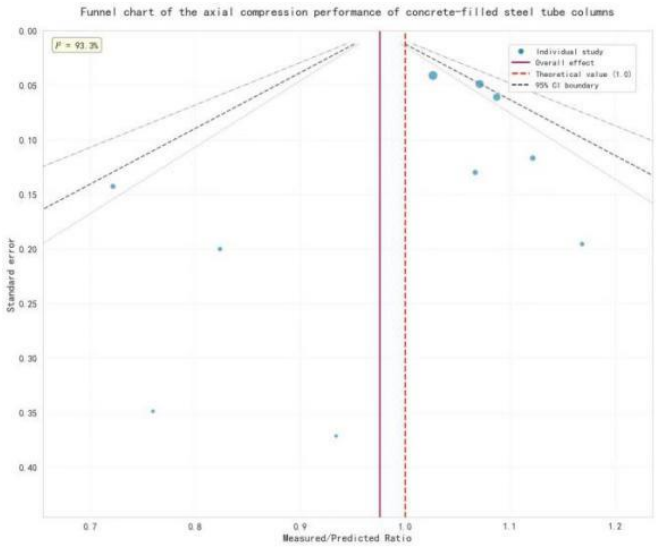

Figure 3. Funnel plot of the influence of cross-sectional shape on N_{ue}/N

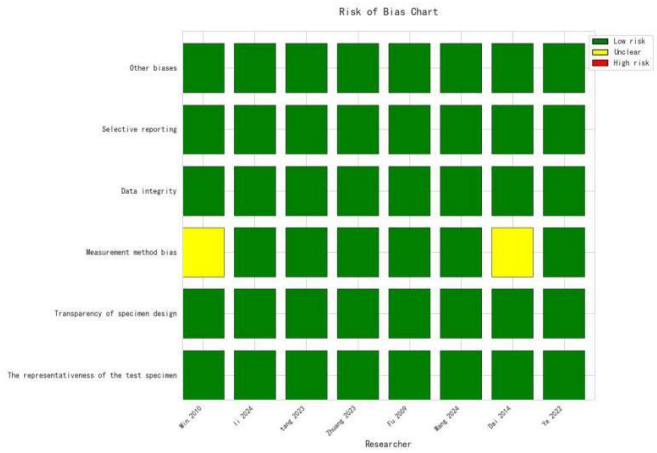

Figure 4. Risk bias diagram

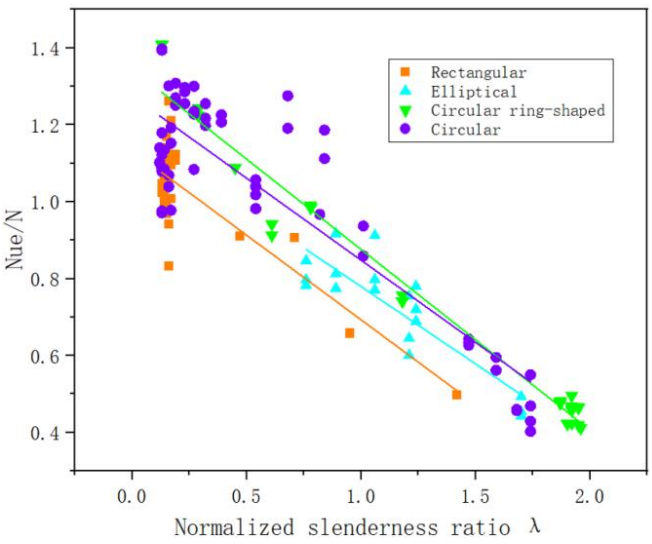

Figure 5. Scatter plot of the sample data and linear regression analysis

3.4 Meta-Analysis of Axial Compression Stability Performance of CFST Columns with Different Cross-Sections

3.4.1 Comparison of Stability Coefficients

The 142 data points were plotted as a scatter plot as shown in Figure 5. Through linear fitting, the linear fitting functions for each section and the stability coefficient at $\lambda = 1$ were obtained, as shown in Table 1. The higher the stability coefficient, the stronger the stability maintaining ability of the column in the slender state[17]. The results show that the stability performance of each section is ranked as follows: circular ring-shaped > circular > elliptical > rectangular. The circular ring-shaped section has the most excellent stability performance in the critical state, which is approximately 26.4% higher than that of the rectangular section.

Table 1. Linear fitting function and the stability coefficient

Cross-section Shape	Linear Fitting Formula	Stability Coefficients(φ=1)
Rectangular	y=-0.44012x+1.13308	0.693
Elliptical	y=-0.40179x+1.18116	0.779
Circular Ring-shaped	y=-0.46954x+1.34538	0.876
Circular	y=-0.42672x+1.27455	0.848

It should also be noted that the absolute values of the slope coefficients of each cross-section are ranked as follows: circular ring-shaped > rectangle > circle > elliptical. This indicates that as the normalized slenderness ratio increases, the stability performance of the circular ring-shaped cross-section prediction model decreases the fastest. After the normalized slenderness ratio exceeds 1.654, its effect is lower than that of the circular cross-section. And the absolute value of the slope coefficients of the elliptical cross-section is the smallest, and its stability performance decreases the slowest as the normalized slenderness ratio increases.

3.4.2 Descriptive Statistics of Corrected Effect Sizes

Table 2 presents the effect size statistics for each cross-section at the $\lambda = 0.657$ reference point. This value directly reflects the accuracy of the existing prediction model in a typical state.

Table 2. The statistical results of the effect size for each cross-section at $\lambda = 0.657$

Cross-section Shape	Sample Size(N)	Mean	Standard Deviation	Median	95% Confidence Interval
Rectangular	42	0.844	0.076	0.839	(0.82099, 0.86677)
Elliptical	18	0.917	0.071	0.910	(0.88456, 0.94978)
Circular Ring-shaped	24	1.078	0.060	1.088	(1.05375, 1.10201)
Circular	58	1.031	0.123	1.027	(0.99971, 1.06309)

The analysis shows that the average effect values for the circular and circular ring-shaped cross-sections are greater than 1, indicating that the measured values are generally higher than the predicted values, and the current design method has a safety margin. Conversely, the average effect values for the rectangular and elliptical cross-sections are less than 1, suggesting that the prediction model may have overestimated their bearing capacity, and there are potential safety hazards.

4. Discussion

This study quantified the influence of cross-sectional shape on the axial compression stability of CFST columns in a unified benchmark, providing a clear and precise assessment.

1. Result interpretation: The circular ring-shaped cross-section combines the advantages of uniform constraints of the circular cross-section and greater external contour stiffness, thus performing well and being reliable in prediction under various aspect ratios. The circular cross-section comes next. The elliptical cross-section has moderate performance. The rectangular cross-section has a weak corner constraint effect and significant stress concentration[18-19], resulting in the lowest stability coefficient and model reliability.

2. Practical significance: In scenarios where the stability of columns is highly demanded, such as in high-rise buildings or large-span structures, circular or circular ring-shaped sections should be preferred. For rectangular cross-sections, designers should be aware of their inferior stability performance and consider using more

conservative stability coefficients or more precise calculation formulas for bearing capacity. The stability coefficient (φ) provided by this study can serve as a reference for performance-based design.

3. Limitation: The linear fitting relationship in this analysis is only valid within a certain range of normalized slenderness ratio, and its extrapolation's general applicability requires further verification.

4. Outlook: This study mainly focuses on regular cross-sections. Since L-shaped, T-shaped and other irregular cross-sections are mostly composed of multiple CFST columns, their force transmission mechanism is different from that of the CFST columns in this study. Therefore, they are not included in the analysis. Their performance analysis requires further systematic research in the future. Future studies can incorporate more parameters such as material strength and diameter-thickness ratio, and establish a more comprehensive design database and multi-parameter prediction model.

5. Conclusion

This study corrected a large amount of data to a unified normalized slenderness ratio and conducted linear fitting analysis. It systematically compared the axial compression stability performance of CFST columns with different cross-sectional shapes. The main conclusions are as follows:

1. Under the unified benchmark ($\lambda = 0.657$), the bearing capacity prediction models for the circular and circular ring-shaped cross-section have higher reliability, while the prediction model for the rectangular cross-section has lower reliability.

2. When reaching the theoretical buckling critical point ($\lambda = 1$), there are significant differences in the stability performance of each cross-section. The strength ranking is: circular ring-shaped > circular > elliptical > rectangular.

3. The comprehensive analysis indicates that the circular cross-section has the best overall performance in terms of axial compression stability. It is recommended that in engineering design and norm revision, this key factor of the cross-sectional shape should be fully considered, and the quantitative conclusions provided in this study should be referred to.

Reference

[1] Schneider, S. P. (1998). Axially loaded concrete-filled steel tubes. *Journal of Structural Engineering*, *124*(10), 1125–1138. https://doi.org/10.1061/(ASCE)0733-9445(1998)124:10(1125

[2] Gourley, B., Tort, C., Haji-Kazemi, H., & et al. (2001). A synopsis of studies on the behavior of concrete-filled steel tube columns. *Canadian Journal of Civil Engineering*, *28*(5), 775–787.

[3] Shams, M., & Saadeghvaziri, M. A. (1997). State of the art of concrete-filled steel tubular columns. *Journal of Constructional Steel Research*, *44*(3), 223–258.

[4] Liberati, A., Altman, D. G., Tetzlaff, J., Mulrow, C., Gøtzsche, P. C., Ioannidis, J. P. A., Clarke, M., Devereaux, P. J., Kleijnen, J., & Moher, D. (2009). The PRISMA statement for reporting systematic reviews and meta-analyses of studies that evaluate health care interventions: Explanation and elaboration. *PLoS Medicine*, *6*(7), Article e1000100. https://doi.org/10.1371/journal.pmed.1000100

[5] Stroup, D. F., Berlin, J. A., Morton, S. C., Olkin, I., Williamson, G. D., Rennie, D., Moher, D., Becker, B. J., Sipe, T. A., & Thacker, S. B. (2000). Meta-analysis of observational studies in epidemiology: A proposal for reporting. *JAMA*, *283*(15), 2008–2012. https://doi.org/10.1001/jama.283.15.2008

[6] British Standards Institution. (2004). *Eurocode 4. Design of composite steel and concrete structures - Part 1-1: General rules and rules for buildings* (EN 1994-1-1:2004).

[7] Wells, G. A., Shea, B., O'Connell, D., Peterson, J., Welch, V., Losos, M., & Tugwell, P. (2011). *The Newcastle-Ottawa Scale (NOS) for assessing the quality of nonrandomised studies in meta-analyses*. Ottawa Hospital Research Institute.

[8] Mander, J. B., Priestley, M. J. N., & Park, R. (1988). Theoretical stress-strain model for confined concrete. *Journal of Structural Engineering*, *114*(8), 1804–1826. https://doi.org/10.1061/(ASCE)0733-9445(1988)114:8(1827

[9] Yu, M., Zha, X. X., Ye, J. Q., & She, C. Y. (2010). A unified formulation for hollow and solid concrete-filled steel tube columns under axial compression. *Engineering Structures*, *32*(4), 1046–1053. https://doi.org/10.1016/j.engstruct.2009.12.031

[10] Li, H. D., Guo, L. H., Gao, S., & Elchalakani, M. (2024). Analysis and design of wide rectangular concrete-filled steel tubular columns under axial compression. *Structures*, *70*, Article 107540.

https://doi.org/10.1016/j.istruc.2024.107540

[11] Tang, H. Y., Qin, J. Y., Liu, Y., & Chen, J. L. (2023). Axial compression behaviour of circular and square UHPC-filled stainless steel tube columns. *Journal of Constructional Steel Research*, *211*, Article 108111. https://doi.org/10.1016/j.jcsr.2023.108111

[12] Zhao, Z., Wei, Y., Wang, G. F., Zhang, Y. R., & Lin, Y. (2023). Axial compression performance of square UHPC-filled stainless-steel tubular columns. *Construction and Building Materials*, *408*, Article 133622. https://doi.org/10.1016/j.conbuildmat.2023.133622

[13] Fu, Z. Q., Ji, B. H., Hu, Z. Q., Wang, R. X., & Wang, W. Z. (2009). Experimental study on behavior of lightweight aggregate concrete-filled steel tube long columns under axial compression. *Journal of Southeast University (Natural Science Edition)*, *39*(3), 546–551.

[14] Wang, Y. B., Song, C., Xiong, M. X., & Liew, J. Y. R. (2024). Mechanical behavior and design applicability of ultra-high-performance concrete-filled circular steel tubular short columns under axial compression. *Engineering Structures*, *299*, Article 117112. https://doi.org/10.1016/j.engstruct.2023.117112

[15] Dai, X. H., Lam, D., Jamaluddin, N., & Ye, J. (2014). Numerical analysis of slender elliptical concrete filled columns under axial compression. *Thin-Walled Structures*, *77*, 26–35. https://doi.org/10.1016/j.tws.2013.11.015

[16] Ye, J. F., Liu, R. Y., Yan, G. Y., Xu, C. S., Li, Y. G., & Li, R. G. (2023). Axial compression behavior of slender circular steel tubular columns filled with geopolymer recycled aggregate concrete incorporating brick aggregates. *Journal of Building Structures*, *44*(5), 264–272.

[17] Chen, W. F., & Lui, E. M. (2005). *Handbook of structural engineering*. CRC Press. https://doi.org/10.1201/9781420039931

[18] Han, L. H., & Yang, Y. F. (2003). Analysis of thin-walled steel RHS columns filled with concrete under uniaxial compression. *Thin-Walled Structures*, *41*(2), 165–189. https://doi.org/10.1016/S0263-8231(03)00029-6

[19] Bradford, M. A., Attard, M. M., & Zhang, L. (2002). Rotational capacity of rectangular concrete-filled steel tube columns. *Journal of Structural Engineering*, *128*(10), 1322–1329.